

## Electronic Supplementary Information (ESI)

### **NIR-II Fluorescence and PA Imaging Guided Activation of STING Pathway in Photothermal Therapy for Boosting Cancer Immunotherapy by Theranostic Thermosensitive Liposomes**

Qi Long<sup>‡a</sup>, Yuliang Yang<sup>‡b</sup>, Fangling Liao<sup>a</sup>, Haoting Chen<sup>a</sup>, Dongyue He<sup>a</sup>, Shengliang  
Li<sup>b</sup>, Pengcheng Li<sup>\*c</sup>, Weisheng Guo<sup>\*a</sup>, and Yafang Xiao<sup>\*a</sup>

<sup>a</sup> Department of Minimally Invasive Interventional Radiology, School of Biomedical  
Engineering & The Second Affiliated Hospital, Guangzhou Medical University,  
Guangzhou, 510260 P. R. China.

*E-mail: [tjuguoweisheng@126.com](mailto:tjuguoweisheng@126.com) (W. Guo); [yafangxiao@gzhmu.edu.cn](mailto:yafangxiao@gzhmu.edu.cn) (Y. Xiao).*

<sup>b</sup> College of Pharmaceutical Sciences, Soochow University, Suzhou 215123, P. R.  
China.

<sup>c</sup> Department of Orthopedics Trauma and Microsurgery, Zhongnan Hospital of  
Wuhan University, Wuhan, Hubei, 430071, P. R. China.

*E-mail: [lpc0730@whu.edu.cn](mailto:lpc0730@whu.edu.cn) (P. Li)*

<sup>‡</sup>Equally contributed: Qi Long and Yuliang Yang

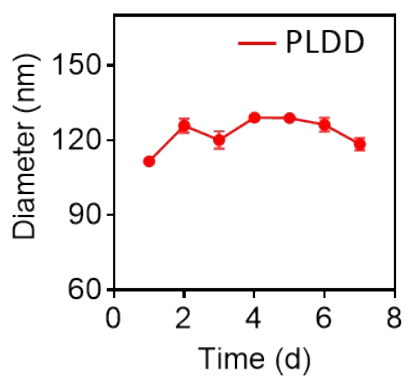


**Fig. S1.** Hydration particle size of PLDD in water for 7 days.

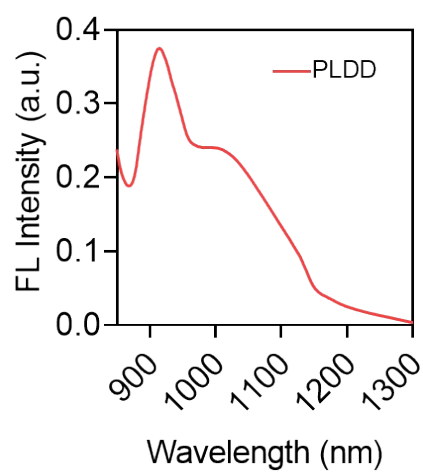


**Fig. S2.** The fluorescence spectra of PLDD in DI H<sub>2</sub>O.

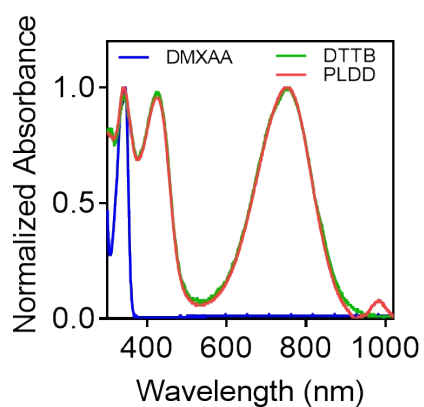


**Fig. S3.** Normalized UV absorption curves of DMXAA, DTTB and PLDD.

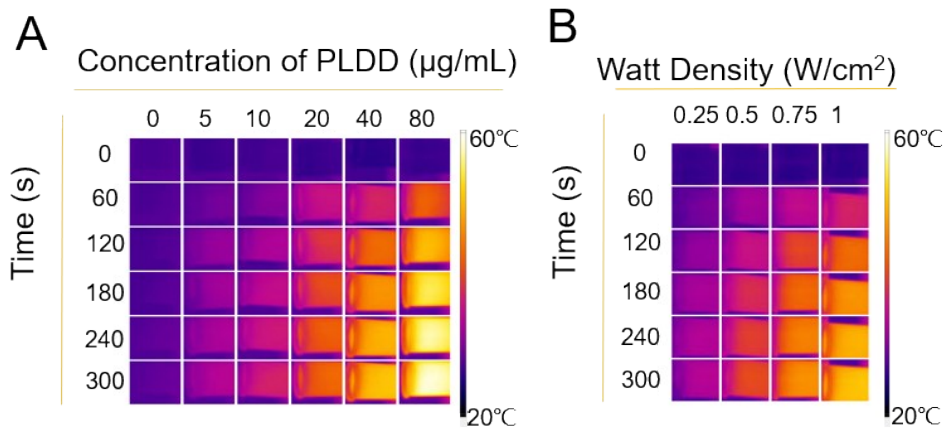


**Fig. S4.** (A) Photothermal maps of different concentrations of PLDD irradiated by an 808 nm laser at a power density of 1 W/cm<sup>2</sup>. (B) Photothermal maps of 808 nm laser irradiation at a concentration of 40 µg/mL of PLDD with different power densities.

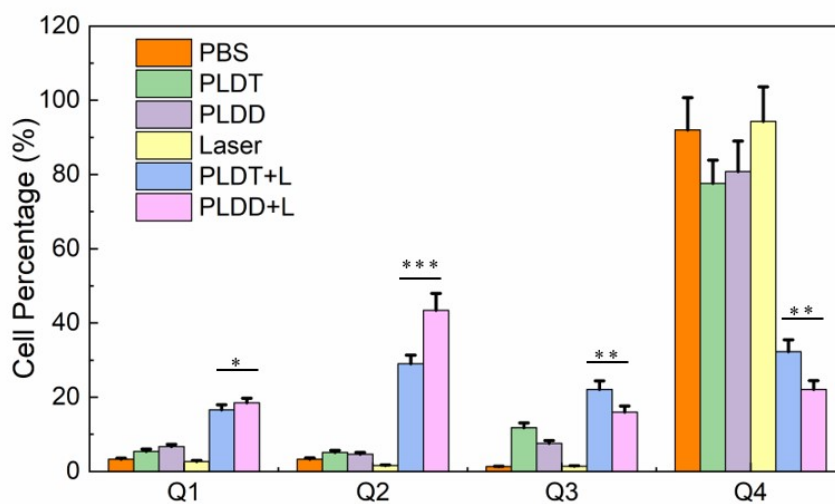


**Fig. S5.** Quantitative analysis of the cell apoptosis by annexin V-FITC/PI Flow cytometry treated with PBS, PLDT, and PLDD in the presence or absence of irradiation. Q1: necrocytosis; Q2: late stage of apoptosis; Q3: early stage of apoptosis; Q4: living cell. (\* $p < 0.05$ , \*\* $p < 0.01$ , \*\*\* $p < 0.001$ )

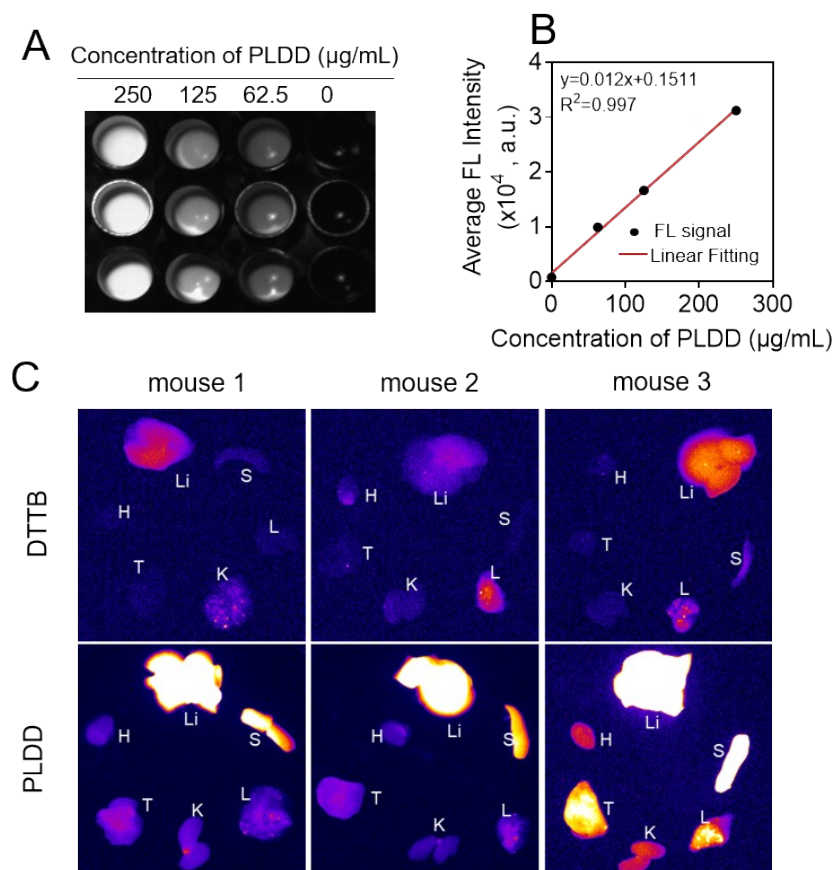


**Fig. S6.** (A) Fluorescence signal plots of different concentrations of PLDD irradiated by an 808 nm laser at a power density of  $60 \text{ mW/cm}^2$  with a 1200 nm long-pass filter and (B) corresponding curves of concentration versus fluorescence intensity. (C) Biodistribution images of DTTB and PLDD in heart (H), liver (Li), spleen (S), lung (L), kidney (K) and tumor (T) distribution by NIR-II fluorescence imaging after 12 h administration.  $n=3$ .

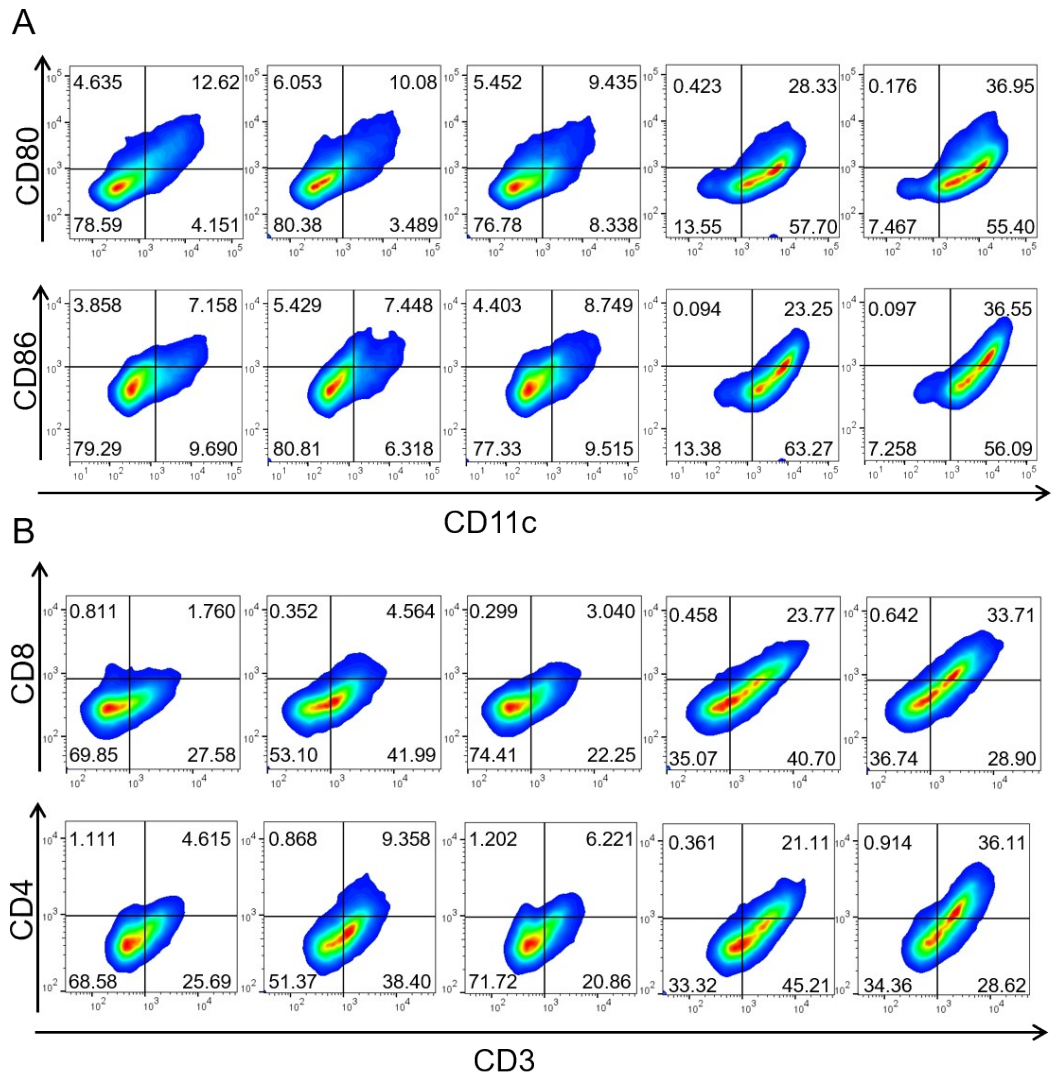


**Fig. S7.** (A) Flow cytometry analysis of CD11c<sup>+</sup>CD86<sup>+</sup> and CD11c<sup>+</sup>CD80<sup>+</sup> content in LLC tumor tissues after treatments. (B) Flow cytometry analysis of CD3<sup>+</sup>CD4<sup>+</sup> and CD3<sup>+</sup>CD8<sup>+</sup> content in LLC tumor tissues after treatments.

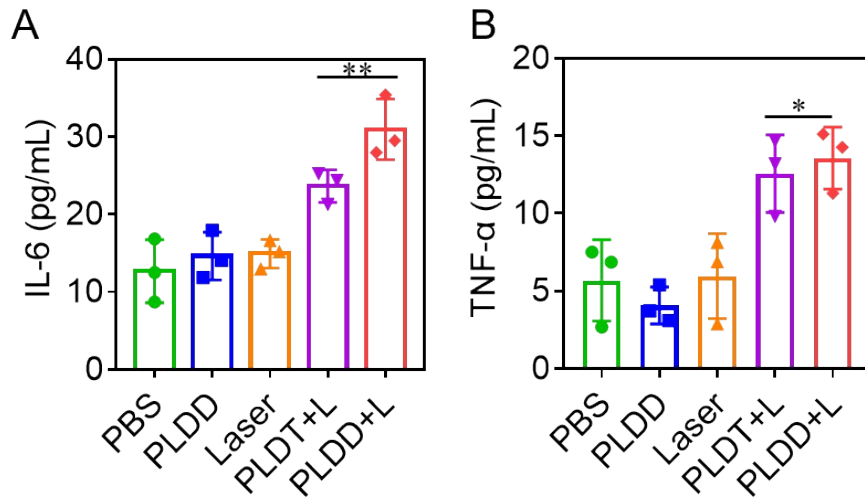


**Fig. S8.** Serum levels of (A) IL-6 and (B) TNF- $\alpha$  in each group of mice after treatments.

(\* $p < 0.05$ , \*\* $p < 0.01$ )